

1 **Supporting Information**

2

3 **Microenvironment Responsive DNA-conjugated Albumin**  
4 **Nanocarriers for Targeting Therapy**

5

6 Jiayu Yu<sup>1,2</sup>, Jianing Zhang<sup>1,2</sup>, Jing Jin<sup>1,\*</sup>, and Wei Jiang<sup>1,2,\*</sup>

7 <sup>1</sup> *State Key Laboratory of Polymer Physics and Chemistry, Changchun Institute of*  
8 *Applied Chemistry, Chinese Academy of Sciences, Changchun 130022, PR China*

9 <sup>2</sup> *University of Science and Technology of China, Hefei, Anhui 230026, PR. China*

10

11 \* Corresponding authors: Fax: +86-431-85262126; Tel: +86-431-85262151

12 *E-mail: [jjin@ciac.ac.cn](mailto:jjin@ciac.ac.cn) (J. Jin); [wjiang@ciac.ac.cn](mailto:wjiang@ciac.ac.cn) (W. Jiang)*

13

14     **Content**

15 S1. Circular Dichroism (CD) Spectroscopy Assay.

16 S2. The Melting Curves Assay.

17 S3. Quantitative analysis of DNA grafting onto BSA surface.

18 S4. TEM images of BSA and DNA-BSA@DOX.

19 S5. Fluorescence intensity standard curve of DOX.

20 S6. DOX Encapsulation Efficiency Assay.

21 S7. Fluorescence spectra of BSA@DOX.

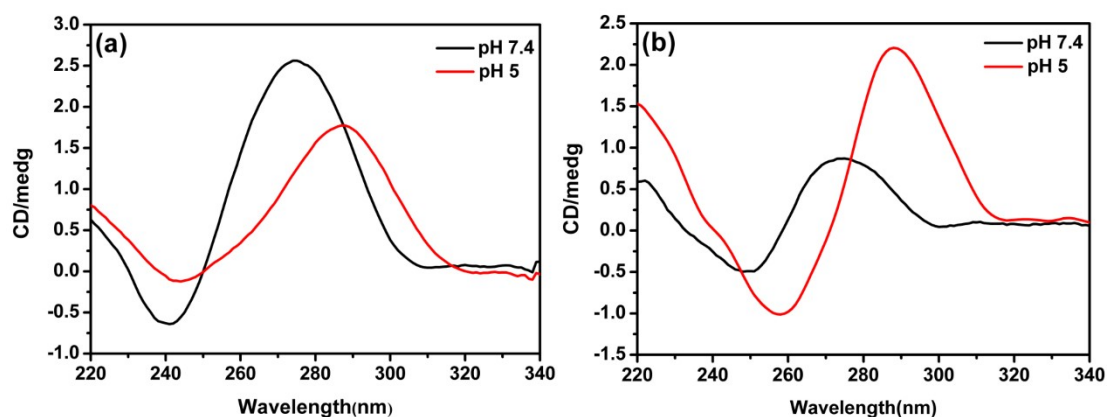
22 S8. Drug loading and release of methylene blue (MB) and daunorubicin (DNR).

23 S9. Hemocompatibility Assay.

24 S10. References.

25

## 26 S1. Circular Dichroism (CD) Spectroscopy Assay



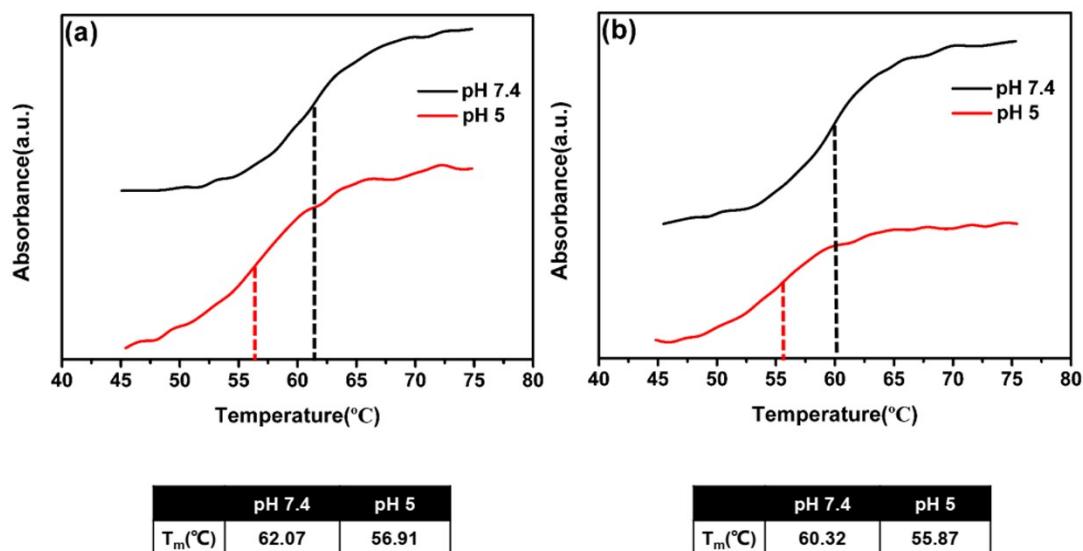
27

28 **Figure S1.** Circular dichroism spectrum of (a) Linker1 and (b) Linker2 in different pH  
29 environments.

30 The pH-responsive drug release is achieved by DNA conformation change.  
31 Circular dichroism(CD) spectropolarimetry was adopted to feedback the information  
32 about conformation change of Linker1 and Linker2 in different pH environments. As  
33 shown in Figure S1, the CD spectrum of Linker1 reveals the negative peak at 240 nm  
34 and the positive peak at 276 nm that implies the formation of G-quadruplex  
35 conformation contrasted to Linker2, an ordinary single-stranded, which the negative  
36 peak at 251 nm and the positive peak at 274 nm in a normal physiological environment  
37 (pH 7.4) and the results are consistent with the previous report.<sup>1</sup> As expected, distinct  
38 changes emerge when the cultured environment is adjusted to sub-acidity (pH 5). The  
39 negative and positive peaks are red-shifted and appear at 244 and 286 nm or 258 and  
40 288 nm for Linker1 and Linker2, respectively, which demonstrate the i-motif structures  
41 are successful in formation.<sup>2, 3</sup> Thus, the pH-responsive conformation changes of the  
42 nanocarriers not only remained stable in the transmission path under a normal  
43 physiology environment but also provided an "OFF-ON" drug delivery performance  
44 triggered by passive targeting (e.g., EPR effect), consequently promoted specific uptake  
45 into the cancer cells.

46

## 47 S2. The Melting Curves Assay



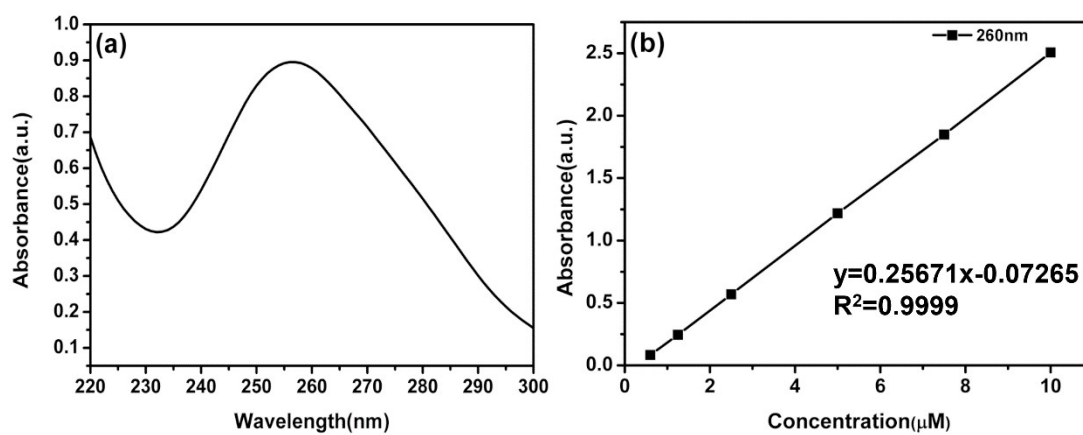
48

49 **Figure S2.** Melt curves of (a) Linker1 hybridized dsDNA and (b) Linker2 hybridized dsDNA at pH  
 50 7.4 and 5 were determined by following changes in the absorbance at 260 nm.

51 The melting curves were determined by following changes in the absorbance at  
 52 260 nm, and the melting temperatures were obtained by taking the maximum of the first  
 53 derivative of the curve. The  $T_m$  of Linker1 hybridized dsDNA (dsDNA1) and Linker2  
 54 hybridized dsDNA (dsDNA2) at pH 7.4 and 5 are shown in Figure S2. At pH 7.4,  
 55 dsDNA1 displays higher  $T_m$  than dsDNA2, which can be attributed to the Linker1  
 56 containing more bases. Whereas at pH 5, the  $T_m$  of both dsDNA1 and dsDNA2 reduce  
 57 about five degrees centigrade, which means the thermal stability of samples is inferior  
 58 to pH 7.4. These two samples' lower  $T_m$  at acidic pH confirms the pH-responsive  
 59 conformation changes and the mechanism triggered by acidic pH. At pH lower than  
 60 6.0, the linkers are formed i-motif structure and dehybridized from dsDNA, and  
 61 simultaneously DBCO-DNA is returned to ssDNA. These results further indicate that  
 62 the nanocarriers possess the pH-responsive capacity.

63

64 **S3. Quantitative analysis of DNA grafting onto BSA surface**



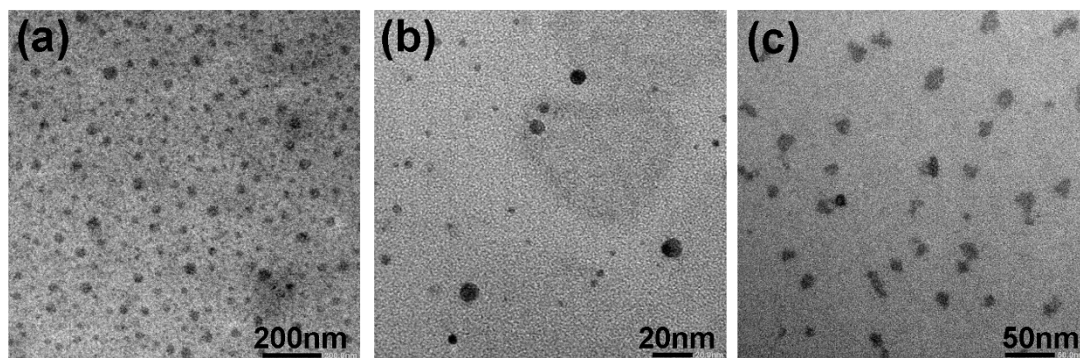
65

66 **Figure S3.** (a) UV-vis absorption spectra of ssDNA-BSA calculated DNA concentration by (b)

67 standard curve of DBCO-DNA between concentration and absorbance at 260 nm.

68

69 S4. TEM images of BSA and DNA-BSA@DOX



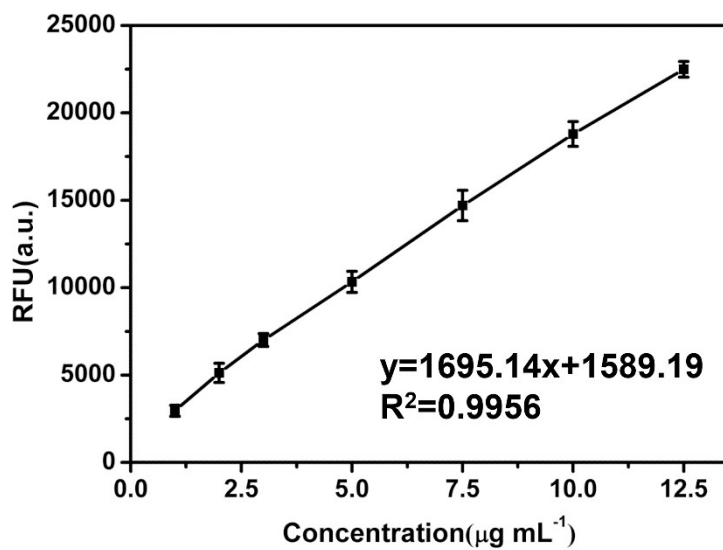
70

71 **Figure S4.** TEM images of (a) BSA, (b) DNA-BSA1@DOX, and (c) DNA-BSA2@DOX.

72

73

74 **S5. Fluorescence intensity standard curve of DOX**



75

76 **Figure S5.** Fluorescence intensity standard curve of DOX with concentration from 1 to 12.5  $\mu\text{g}$

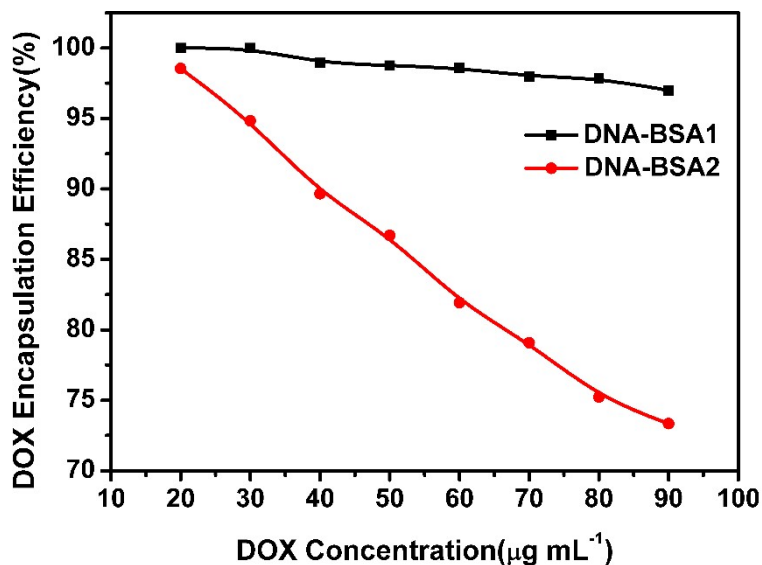
77  $\text{mL}^{-1}$ .

78

79

80 **S6. DOX Encapsulation Efficiency Assay**

81 To load the drug into the nanocarriers, a mixture of DOX solution (from 20 to 90  
82  $\mu\text{g mL}^{-1}$ ) with DNA-BSA solution ( $1 \mu\text{M}$ ) was reacted at room temperature for 40min.  
83 Then, 100  $\mu\text{L}$  of the sample was added to 96-well plates. The fluorescence spectra of  
84 DOX (excitation, 480 nm; emission, 595 nm) was measured by a microplate reader  
85 (Bio-Tek).

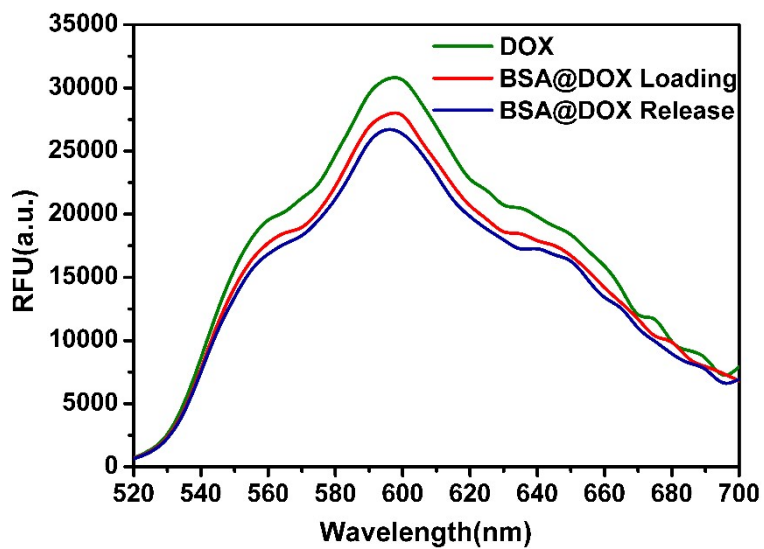


86  
87 **Figure S6.** The DOX encapsulation efficiency of DNA-BSA1 and DNA-BSA2 at different feeding  
88 concentrations with a constant nanocarriers concentration ( $1 \mu\text{M}$ ).

89



90 S7. Fluorescence spectra of BSA@DOX



91

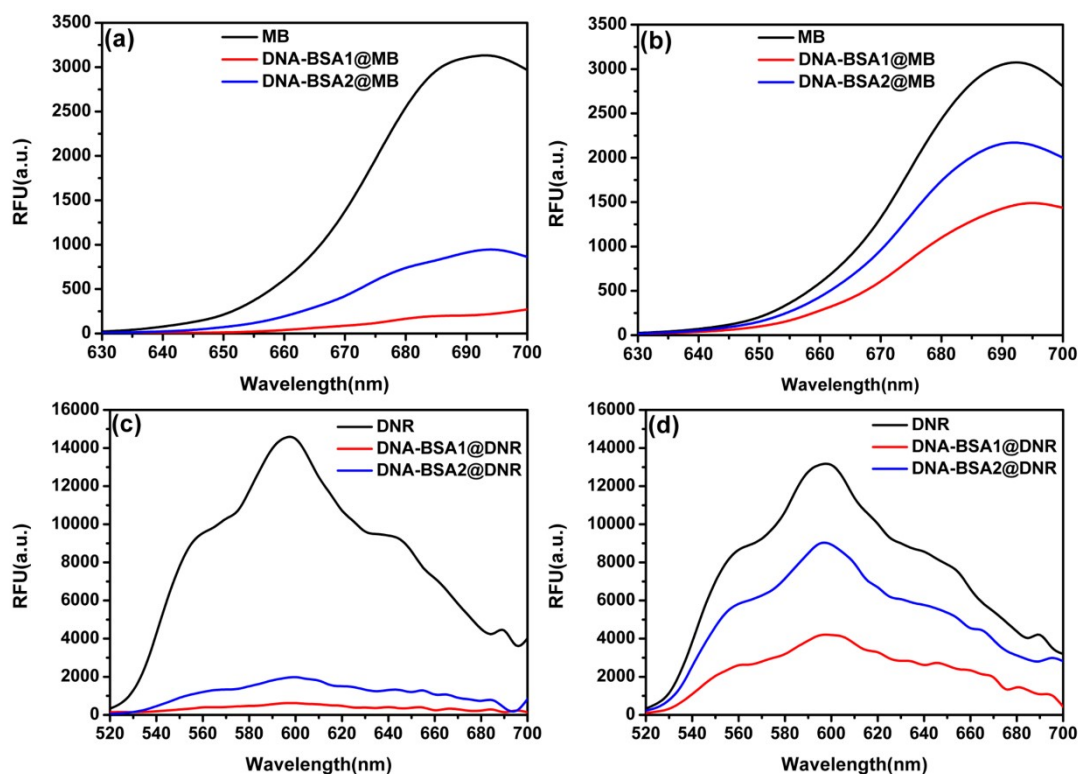
92 **Figure S7.** Fluorescence spectra of BSA@DOX loading and release by changing pH value.

93

94 **S8. Drug loading and release of methylene blue (MB) and daunorubicin (DNR)**

95 To load the drug into the nanocarriers, mixtures of DNA-BSA solution (1  $\mu\text{M}$ ) with  
96 MB or DNR solution (20  $\mu\text{g mL}^{-1}$ ) were reacted at room temperature for 40min. Then,  
97 100  $\mu\text{L}$  of the sample was added to 96-well plates, and the fluorescence spectra (MB:  
98 excitation, 600 nm, emission, 695 nm; DNR: excitation, 480 nm, emission, 595 nm)  
99 were measured by a microplate reader (Bio-Tek).

100 To investigate pH-triggered drug release behavior from DNA-BSA nanocarriers,  
101 drug-loaded nanocarriers were diluted with PBS buffer (pH 5.0) to final concentration  
102 at 500 nM and DOX concentration at 10  $\mu\text{g mL}^{-1}$ . After that, incubated at 37  $^{\circ}\text{C}$ , the  
103 released DOX was recorded by the above-mentioned method.

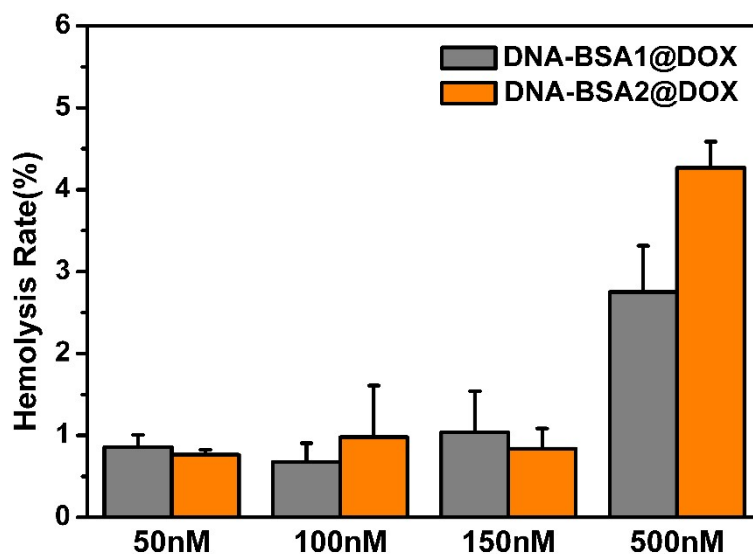


104

105 **Figure S8.** Fluorescence spectra of MB (a) or DNR (c) loading into DNA-BSA1 and DNA-BSA2

106 and release (b) or (d) under acid condition.

107 **S9. Hemocompatibility Assay**



108

109 **Figure S9.** Hemolysis rates of DNA-BSA@DOX with different concentrations.

110 Outstanding biocompatibility and hemocompatibility are the important  
111 characteristics of biomedical nanomaterials. Thus we performed a hemolysis analysis  
112 to evaluate as-prepared nanocarriers. As shown in Figure S7, nanocarriers with  
113 concentrations from 0-500 nM do not display an obvious hemolytic effect (< 5%) and  
114 correspond to threshold values reported in the previous literature.<sup>4</sup> Thus, DNA-  
115 BSA1@DOX and DNA-BSA2@DOX display excellent biocompatibility, on this  
116 premise, provide a great guarantee for cancer treatments.

117

118 **S10. References**

- 119 1. A. Rajendran and B. U. Nair, *Biochimica Et Biophysica Acta-General*  
120 *Subjects*, 2006, **1760**, 1794-1801.
- 121 2. J. Choi, S. Kim, T. Tachikawa, M. Fujitsuka and T. Majima, *Journal of the*  
122 *American Chemical Society*, 2011, **133**, 16146-16153.
- 123 3. A. Rajendran, S.-i. Nakano and N. Sugimoto, *Chemical Communications*,  
124 2010, **46**, 1299-1301.
- 125 4. Q. Chen, H. Wang, H. Liu, S. Wen, C. Peng, M. Shen, G. Zhang and X. Shi,  
126 *Analytical Chemistry*, 2015, **87**, 3949-3956.

127